Pre-Clinical Research Report

Journal of INTERNATIONAL MEDICAL RESEARCH

Journal of International Medical Research
2018, Vol. 46(7) 2843–2855

DOI: 10.1177/0300060518774687
journals.sagepub.com/home/imr
SAGE

Lens-specific deletion of the *Msx2* gene increased apoptosis by enhancing the caspase-3/caspase-8 signaling pathway

Ziyan Yu[1,2,#], Wenting Yu[1,#], Jia Liu[1], Danhong Wu[3], Chunxia Wang[1], Jinsong Zhang[1] and Jiangyue Zhao[1]

Abstract

Objective: To investigate the influence of *Msx2* conditional gene knockout during lens development in mice.

Methods: Lens-specific *Msx2* knockout mice were generated using the *Cre*-loxP system. The eyes of *Msx2* conditional knockout (*Msx2*CKO) and wild-type (*Msx2*WT) mice were examined during embryonic and early postnatal periods using histological, immunofluorescence, *in situ* hybridization, cell proliferation, apoptosis, and mRNA microarray analyses.

Results: *Msx2*CKO mice exhibited small lens formation and microphthalmia after birth, while *Msx2*CKO embryos exhibited a persistent lens stalk, small lens formation, and microphthalmia. Conditional deletion of *Msx2* also led to an increased apoptosis rate, a significant reduction in *FoxE3* expression, and an upregulation of *Prox1* expression in the lens vesicle during the early embryonic period. Microarray comparison of *Msx2*CKO and *Msx2*WT lens transcriptomes identified a large number of differentially expressed genes. Real-time PCR showed that *Casp8* and *Casp3* expression was upregulated in *Msx2*CKO mice at post-natal day 1.

Conclusion: The activation of apoptosis through the caspase-8/caspase-3 signaling pathway, together with the downregulation of *FoxE3* expression, appeared to account for the smaller lens formation in *Msx2*CKO mice.

[1]Department of Ophthalmology, Fourth Affiliated Hospital of China Medical University, Eye Hospital of China Medical University, Provincial Key Laboratory of Lens Research, Shenyang, China
[2]Keck School of Medicine, University of Southern California, Los Angeles, CA, USA
[3]Department of Neurology, Shanghai Fifth People's Hospital, Fudan University, Shanghai, China
[#]These authors contributed equally to this work.

Corresponding author:
Jiangyue Zhao, 11 Xinhua Road, Shenyang 110004, China.
Email: zhaojiangyue@hotmail.com

Keywords
Msx2, apoptosis, FoxE3, lens development, Casp3, Casp8

Date received: 12 January 2018; accepted: 12 April 2018

Introduction

The lens is a sensory organ that transmits and focuses light onto the retina. In vertebrates, the head surface of the embryo ectoderm develops into the lens.[1–3] Homeobox genes function as essential transcriptional regulators in a variety of developmental processes.[4] *Msx* genes encode members of the muscle segment homeobox gene family, including *Msx1*, *Msx2*, and *Msx3*, which are three unlinked members sharing 98% homology in their homeodomain.[5] *Msx2* is expressed at sites of epithelial–mesenchymal interaction during embryogenesis.[6–13] Its encoded protein is both a transcriptional repressor and activator whose normal activity may establish a balance between survival and apoptosis, and could also promote cell growth under certain conditions.[5,9,12,14,15]

Previous evidence revealed that low levels of *Msx2* expression were present in the developing murine optic vesicle,[16,17] while *Msx1*/*Msx2* double-null mutants showed arrested eye development.[18] We previously demonstrated that *Msx2* functions as an apoptosis-promoting factor in the developing murine optic vesicle; overexpression of the *Msx2* transgene in mice resulted in optic nerve aplasia and microphthalmia.[19] Germline knockouts ($Msx2^{-/-}$) exhibited small lens formation or even aphakia, as well as a persistent lens stalk and iris hyperplasia in the anterior segment.[14] $Msx2^{-/-}$ mice also previously showed retina folding and microphthalmia.[14]

Genetic evidence has indicated that lens formation depends on retinal formation in mice,[20–23] and Pax6 was identified as a key regulator of early eye development. However, to further understand the Msx2 function in controlling embryonic lens development and to exclude the retinal influence on lens development through formation of the optic cup or gene expression in $Msx2^{-/-}$ mice, we produced *Msx2* conditional knockout mice (*Msx2*CKO) using the *Le-Cre* mouse line.[24] Comparative histological and gene expression analyses were performed to trace morphological and genetic changes and to identify molecular pathways associated with lens development.

Materials and methods

Animal model establishment

Mice homozygous for a floxed allele of *Msx2* ($Msx2^{fl/fl}$) were provided by Professor Benoît Robert (Pasteur Institute, Paris, France). *Pax6* promoter-driven *Cre* transgenic mice (*Le-Cre* mice) were obtained from Professor David Beebe (Washington University, St, Louis, MO) with permission from Dr Peter Gruss (Max Planck Institute for Biophysical Chemistry, Göttingen, Germany), and Professor Ruth Ashery-Padan (Tel Aviv University, Tel Aviv, Israel).[24] *ROSA26R* mice were purchased from the Jackson laboratory.[25] All mice were housed and cared for in accordance with the National Institutes of Health guide for the care and use of laboratory animals, and regulations set by the University of Southern California and China Medical University. The study protocol was approved by the ethics

committee of China Medical University (16005M).

Our mating scheme generated mice that were homozygous for the floxed allele (*Msx2*$^{fl/fl}$) and were either *Le-Cre*-positive (*Le-Cre*;*Msx2*$^{fl/fl}$;*Msx2*CKO) or *Le-Cre*-negative (*Msx2*$^{fl/fl}$, *Msx2*WT) as littermate controls (Figure 1a). Male mice carrying the *Le-Cre* allele were crossed with females carrying the *R26R* conditional reporter allele to generate *Le-Cre;R26R* embryos (time-staged embryos expressing a *lacZ* reporter gene). Genotyping was performed by PCR using primers for *Cre* recombinase (forward: 5′-TAATCGCCATCTTCCAGC AG-3′ and reverse: 5′-CTCTGGTG TAGCTGATGATC-3′) and floxed alleles of *Msx2* (forward: 5′-GTTGAGCCGAG TCTCCCACCT-3′ and reverse: 5′-GAT TCCTTGGGCGGCTTCTT-3′). PCR conditions to amplify *Cre* were: 94°C for 4 minutes, then 35 cycles of 94°C for 1 minute and 60°C for 1 minute, followed by 72°C for 1 minute, and 4°C for 10

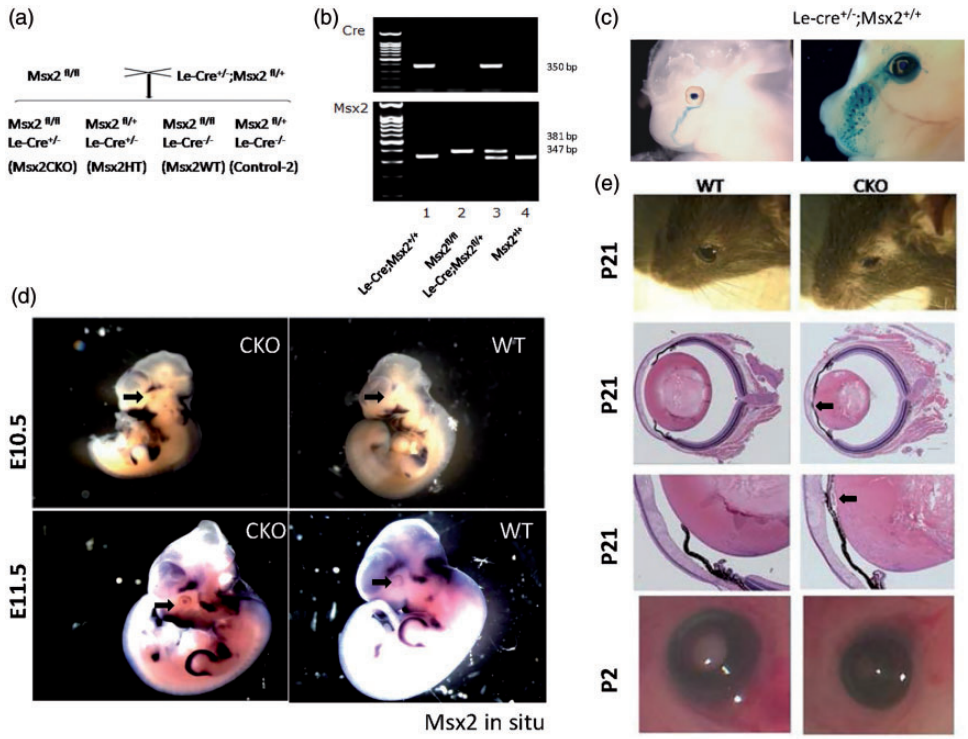

Figure 1. Generation of *Msx2*CKO mice. (a) Mating scheme. (b) Genotyping performed by PCR. The 350 bp band represents Le-Cre; the 347 bp band represents the wild-type; and the 381 bp band represents the mutant. (c) The recombination pattern of *Le-Cre* was detected by β-galactosidase whole mount staining at E10.5 and E14.5. (d) Whole mount *in situ* hybridization showing the absence of *Msx2* mRNA in the *Msx2*CKO lens vesicle at E10.5 and E11.5. (e) *Msx2*CKO mice lacked eyelashes and hair on the surface of their eye lids and in a stripe running from the temporal to the nasal side of the eye ($n \geq 3$ per genotype) at P21. *Msx2*CKO mice showing reduced lens size and microphthalmia at P2. Histological sections of the *Msx2*CKO eyeballs showing reduction in the lens size, displacement of lens fiber nuclei toward the anterior and posterior of the lens, and vacuolation of cortical fiber cells at P21.

minutes. PCR conditions to amplify *Msx2* were the same but amplification was carried out at 56°C rather than 60°C.

RNA microarray analysis

Total RNA was extracted from lenses isolated from *Msx2*CKO (n = 3) and *Msx2*WT mice (n = 3) on day P1 using an RNeasy micro kit (Qiagen GmbH, Hilden, Germany). *Msx2*WT lenses were used as controls. The microarray was carried out by Shanghai Biotechnology Corporation (Shanghai, China) using one-color microarray-based gene expression analysis. Microarray data and protocols have been submitted to NCBI's Gene Expression Omnibus (GEO) database at http://www.ncbi.nlm.nih.gov/geo with a GEO accession number of GSE92947.

Differentially expressed genes (DEGs) were identified using online SBC Analysis System (SAS) statistical software (http://sas.shbio.com/). To identify the functions of DEGs, gene ontology (GO) and KEGG pathway enrichment analyses were carried out using online SAS software.[26] Cytoscape ClueGO software (National Institute of General Medical Sciences, Bethesda, MD, USA) was used for DEG molecular function analysis.

Real-time quantitative PCR of lens tissue

RNA specimens were extracted from the lenses of three *Msx2*CKO and three *Msx2*WT mice at post-natal day (P)1 using the RNeasy micro kit (Cat#74004; QIAGEN GmbH). Quantitative PCR was carried out to verify the microarray results by amplifying *Casp8* and *Casp3* using primers forward: 5′-CCACGAGATT CTAGAAGGCTACCAAAGCGC-3′ and reverse: 5′-CTCACGTCATAGTTCACG CCAGTCA-3′, and forward: 5′-CCAT GGTGAAGGGGTCATTTATGGGACA-3′ and reverse: 5′-TGGACACAATACAC GGGATCTGTTTCTTTG-3′, respectively. PCR included SYBR Premix Ex Taq™ II (Takara, Dalian, China), and conditions were 94°C for 2 minutes, followed by 40 cycles of 94°C for 1 minutes and 60°C for 40 s. Results were analyzed using the equation $RQ = 2^{-\Delta\Delta CT}$.

β-galactosidase whole mount staining

Time-staged embryos expressing the *lacZ* reporter gene were fixed with 1% paraformaldehyde and stained at 37°C in the dark overnight by immersion in 1 mg/mL X-gal staining solution (https://www.jax.org/research-and-faculty/tools/cre-repository/whole-mount-staining-protocol).[10,27]

Whole mount in situ *hybridization*

Time-staged embryos were fixed overnight in 4% paraformaldehyde in phosphate-buffered saline. Whole-mount *in situ* hybridization was performed using standard protocols.[28] The *Msx2* cDNA plasmid was purchased from the ATCC (Manassas, VA, USA). *FoxE3* plasmids were kindly provided by Peter Carlsson (University of Gothenburg, Gothenburg, Sweden). Msx2 and FoxE3 RNA probes were labeled with digoxigenin-UTP according to the manufacturer's recommendations (Roche, Basel, Switzerland).

Histological analysis

Embryos between E9.5 to E16.5 and eyeballs at P2 and P21 were fixed overnight in Davidson's fixative solution (glacial acetic acid:95% ethyl alcohol:10% neutral buffered formalin: distilled water 1:3:2:3). They were then dehydrated through a graded alcohol series, cleared in xylene, and embedded in paraffin. Sections were cut to 5 μm, then stained with hematoxylin and eosin. Lens size was quantified by measuring the anteroposterior and horizontal

diameters in both groups from E9.5 to E12.5.

Immunohistochemistry

After deparaffinization and rehydration, sections were boiled for 10 minutes in antigen repair solution, then blocked with 5% bovine serum albumin for 1 hour. They were incubated with the primary antibodies anti-Sox2 (Santa Cruz Biotechnology, Santa Cruz, CA, USA), anti-Pax6 (University of Southern California, Los Angeles, CA), anti-AP2-α (University of Southern California), and anti-N-cadherin and anti-E-cadherin (kindly provided by Dr Yue Zhao, China Medical University). Sections were then incubated with fluorescent-labeled secondary antibodies DyLight™ 549-conjugated donkey anti-mouse IgG and DyLight™ 488-conjugated donkey anti-rabbit IgG (Jackson ImmunoResearch Laboratories, Inc., West Grove, PA, USA) at room temperature for 2 hours. Cell nuclei were counterstained with 4′,6-diamidino-2-phenylindole. Sections (5 μm) were mounted and viewed under a fluorescence microscope (Zeiss, Gottingen, Germany).

5-bromo-2′-deoxyuridine (BrdU) staining

Pregnant mice were sacrificed at various time points after conception. One h before sacrifice, the mice were injected intraperitoneally with 100 μg BrdU (Sigma, St. Louis, MO, USA) per gram of body weight. A BrdU kit was used (Roche), and cell counting was conducted according to a modified protocol.[14]

Terminal deoxynucleotidyl transferase dUTP nick end labeling assay

Apoptotic cells were detected using the fluorescein *in situ* Cell Death Detection Kit (Roche Applied Science, Indianapolis, IN, USA).[29] Labeled cells were visualized with a fluorescence microscope and images were captured.

Statistical analyses

Statistical evaluations between control and mutant samples were performed using one-way analysis of variance. A P-value < 0.05 indicated that the observed differences were statistically significant.

Results

Rise in small lens formation from the conditional deletion of Msx2

We generated *Msx2*CKO and *Msx2*WT mice, and genotyped them using PCR (Figure 1a, 1b). The temporal and spatial activity of *Le-Cre* was characterized by whole mount β-galactosidase staining (Figure 1c).[25] We detected *Msx2* transcripts by whole mount *in situ* hybridization beginning on E9 (data not shown). As early as E10.5, the *Msx2*CKO lens placode failed to detect any signals, suggesting that *Msx2* lost its function at this time. A weak hybridization signal for *Msx2* was observed in the dorsal retina and lens vesicle in *Msx2*WT mice (Figure 1d). The *Msx2*CKO lens placode also failed to detect any signals in the lens vesicle stage (E11.5) (Figure 1d). Noteworthy differences were observed between *Msx2*CKO and *Msx2*WT mice on gross inspection. At P2, *Msx2*CKO mice exhibited a small lens size and microphthalmia. At P21, *Msx2*CKO mice again showed a small lens size, as well as bilateral microphthalmia, smaller corneas, missing eyelashes and fur between the eyes and snout, lens fiber nuclei displaced towards their anterior and posterior aspects, and vacuolated fiber cells (Figure 1e).

Differences in developing eye specimens were also observed between *Msx2*CKO and their wild-type littermates. At E9.5, no significant difference was observed between

the developing eyes of *Msx2*CKO and *Msx2*WT embryos (Figure 2a). By contrast, defects in the lens were evident as early as E10 and E10.5. At this stage, the lens vesicle was considerably smaller in *Msx2*CKO embryos (Figure 2a). At E11.5, the lens vesicle appeared smaller and was surrounded by neurilemma cells in the *Msx2*CKO group (Figure 2a). At E12.5, the lens vesicle epithelium was completely separated from

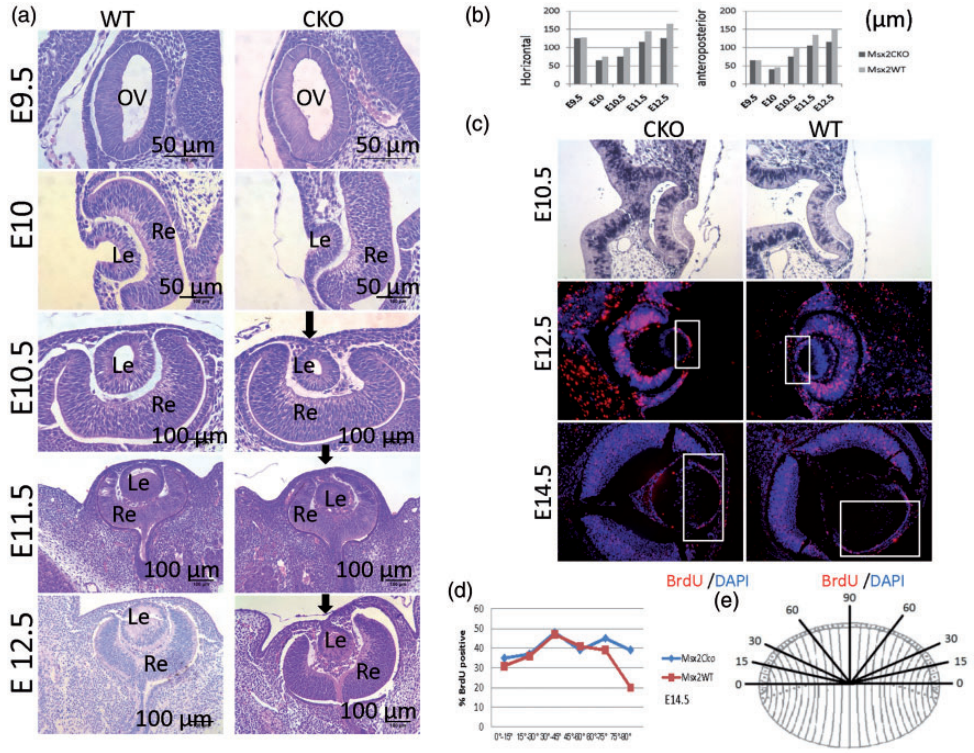

Figure 2. (a) HE staining. At E9.5, the optic vesicle (OV) is in contact with the lens placode and no structural differences are observed between *Msx2*CKO and *Msx2*WT embryos. At E10.5, the lens vesicle that had invaginated into the optic cup is considerably larger in the developing eyes of *Msx2*WT mice. At E11.5, the lens vesicle has closed in the eyes of both *Msx2*WT and *Msx2*CKO mice, but appears smaller in *Msx2*CKO embryo. At E12.5, the epithelium of the lens vesicle has completely separated from the surface ectoderm in *Msx2*WT mice, but remains adherent in *Msx2*CKO mice. Black arrow: lens stalk. Re, Retina; Le, Lens; Co, Cornea. OV, optic vesicle. (b) Column diagram of the horizontal lens diameter (left) and anteroposterior diameter (right) of *Msx2*CKO and *Msx2*WT mice between E9 and E12.5. Significant differences from E10.5 to E12.5 were observed between the two groups ($P<0.05$). (c) Altered cell proliferation. At E10.5, no differences were observed in the ratio of BrdU-positive lens cells between *Msx2*CKO and *Msx2*WT mice. At E12.5, the absolute number of lens epithelia incorporating BrdU was significantly reduced in *Msx2*CKO mice compared with *Msx2*WT mice, but the ratio of BrdU-positive cells was virtually identical. (d) At E14.5, the BrdU labeling rate in lens epithelial cells was the lowest in the 0° to 15° sector in both *Msx2*CKO and the *Msx2*WT mice. The ratio of BrdU-positive cells in the 60°–90° sectors was significantly increased in central lens epithelial cells in *Msx2*CKO mice compared with *Msx2*WT mice; no difference was found in the 15°–45° sectors in *Msx2*CKO mice compared with *Msx2*WT mice. (e) Cell counting method. Schematic of the division of lens epithelia (LE) into 15 sections showing the location of the transition zone (0°–15°) and the germative zone (15°–30°) of the LE and the lens fiber (LF) compartment.

the surface ectoderm in *Msx2*WT embryos, while it remained adherent in *Msx2*CKO mice (Figure 2a). Subsequently at E14.5 and E16.5, *Msx2*CKO embryo eyes were greatly reduced in size and the cornea and lens had not separated, whereas the lens vehicle had completely separated from the surface ectoderm of *Msx2*WT littermates, and epithelial cells at the equator of the lens were disorganized (Figure S1). Significant differences in the horizontal lens diameter and anteroposterior diameter were observed between the two groups from E10.5 to E12.5 ($n = 6$, $P < 0.05$), but not at E9.5 and E10 ($n = 6$) (Figure 2b).

Changes in cell proliferation

To assess whether cell proliferation was involved in small lens formation, embryos were examined using *in vivo* BrdU labeling (Figure 2c, 2e). At E10.5, no differences were observed in the ratio of BrdU-positive cells between *Msx2*CKO and *Msx2*WT mice ($n = 4$). At E12.5, *Msx2*CKO mice showed smaller lens vesicles, and the absolute number of lens cells that incorporated BrdU was significantly reduced compared with wild-type littermates ($P < 0.05$), but the ratio of BrdU-positive cells was virtually identical ($n = 4$). We also evaluated the proliferation rate at E14.5, a relatively late stage of lens development when cells begin to withdraw from the cell cycle in preparation for fiber cell terminal differentiation. The BrdU labeling rate in lens epithelial cells was lowest in the 0° to 15° sector in both *Msx2*CKO and *Msx2*WT mice, with no significant difference between the two groups at E14.5 (Figure 2d). The ratio of BrdU-positive cells in 60°–90° sectors was found to be significantly increased in central lens epithelial cells at E14.5 in *Msx2*CKO mice compared with *Msx2*WT mice ($n = 4$, $P < 0.01$); no significant difference was found in 15°–45° sectors at E14.5 in *Msx2*CKO mice compared with *Msx2*WT mice ($n = 4$) (Figure 2d).

Increased apoptosis

At E10.5, a significantly higher level of lens epithelial cell (LEC) apoptosis was observed in *Msx2*CKO embryos that was mainly concentrated near the lens stalk ($n = 4$, $P < 0.05$) (Figure 3a). From E12.5 to E16.5, very few apoptotic LECs were observed in *Msx2*WT mice, but the absolute number of apoptotic LECs was significantly increased in *Msx2*CKO mice compared with *Msx2*WT littermates ($n = 4$, $P < 0.01$) (Figure 3b, 3c). Additionally, our *in vitro* study found that small interfering RNA knockdown of *Msx2* in cultured murine α-TN4 cells increased the apoptosis rate of murine LECs in by over 3-fold (data not shown).

Enhanced Casp3/Casp8 signaling pathway affecting lens development

Microarray analysis showed there were 3412 DEGs with a greater than 2-fold change in expression in the *Msx2*CKO lens compared with the *Msx2*WT lens; of these, 1815 genes were upregulated and 1597 were downregulated (Figure 4a). Members of apoptosis signaling pathways, caspase 3 (*Casp3*) and caspase 8 (*Casp8*), were shown to be upregulated in the *Msx2*CKO lens compared with the *Msx2*WT lens (Figure 4a). KEGG pathway enrichment analysis, GO enrichment analysis, and molecular function ClueGO analysis were performed (Figure S2).

Real-time quantitative PCR was performed to detect the expression levels of apoptosis-related markers at P1; the expression of *Casp3* and *Casp8* was significantly increased in *Msx2*CKO lenses compared with *Msx2*WT controls ($P < 0.05$; Figure 4b).

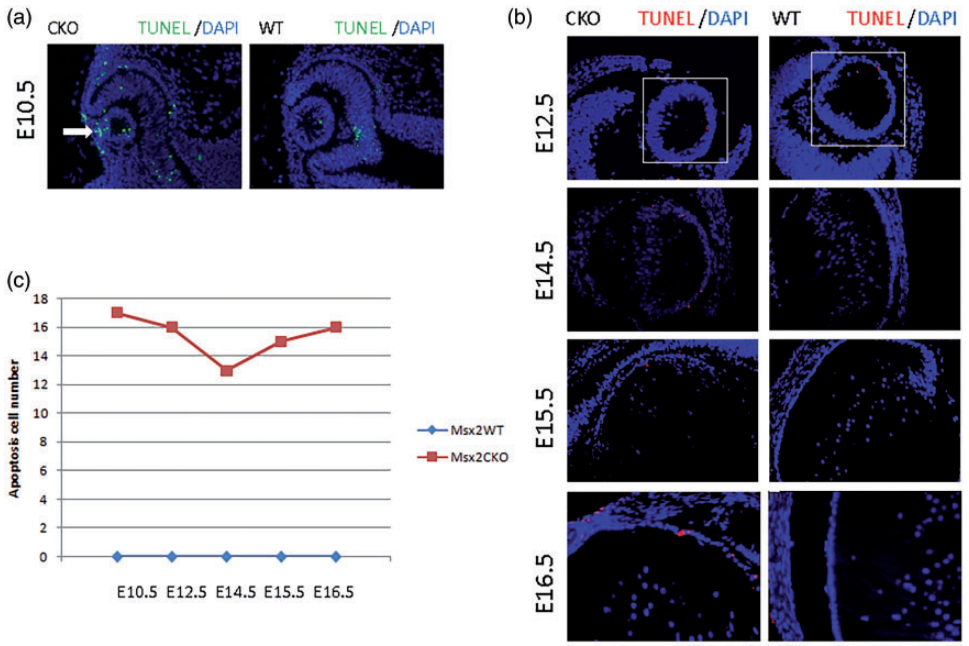

Figure 3. (a) At E10.5, a significantly higher level of lens epithelial cell apoptosis was observed that was mainly concentrated near the lens stalk in *Msx2*CKO embryos. (b, c) From E12.5 to E16.5, very few apoptotic lens epithelial cells were observed in *Msx2*WT mice, but the absolute number of lens epithelial cells undergoing apoptosis was significantly increased in *Msx2*CKO mice compared with *Msx2*WT mice.

Alterations in FoxE3 *and* Prox1 *expression in* Msx2*CKO mice*

The intensity and distribution of Pax6, Sox2, and AP2α transcription factors in *Msx2*CKO embryos were identical to their wild-type counterparts at E10.5 (Figure S3). Whole mount *in situ* hybridization revealed a dramatic reduction in *FoxE3* expression at E10.5 in the lens pit of *Msx2*CKO embryos compared with wild-type littermates (Figure 4c). At E11.5, *FoxE3* expression in the anterior lens epithelium of *Msx2*CKO embryos remained lower than in wild-type littermates (Figure 4d). Immunostaining of *Prox1* expression was significantly increased in the lens vehicles of *Msx2*CKO embryos compared with wild-type littermates at E11.5 (Figure S3). At E14.5, the intensity of N-cadherin and E-cadherin expression in the anterior lens epithelium was identical in *Msx2*CKO and *Msx2*WT embryos (Figure S3).

Discussion

In this study, we observed that *Msx2*CKO mice exhibited small lens formation, lens stalk persistence, displaced lens fiber nuclei, and vacuoles in their cortical fiber cells compared with WT littermates. These abnormal phenotypes are similar to those observed in $Pax6^{Sey/+}$, $Sox11^{-/-}$, $FoxE3^{-/-}$, and $Msx2^{-/-}$ mice.[14, 30–32] Microarray analysis and real-time PCR provided evidence that *Casp3*/*Casp8* are activated and that the apoptosis caspase signaling pathway might participate in lens apoptosis of *Msx2*CKO mice.

Whether the lens formation depends on retina formation is one of the oldest questions in ocular development.[20,21] $Msx2^{-/-}$

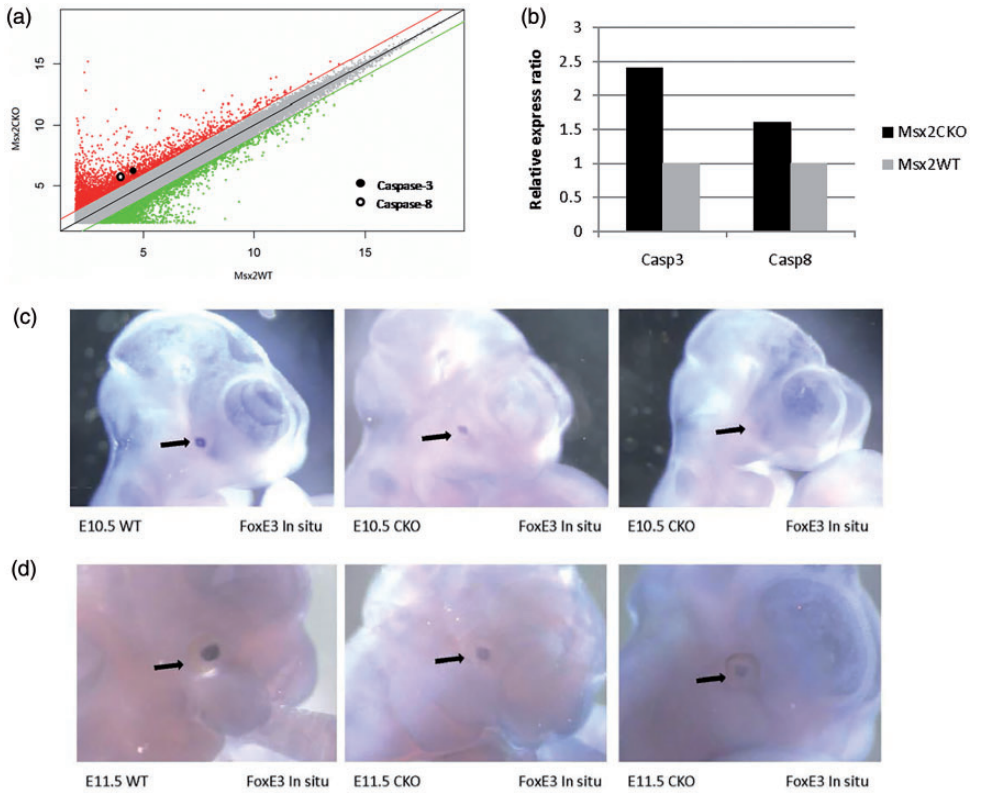

Figure 4. (a) RNA microarray and differentially expressed gene analysis. Scatter plot showing upregulated genes (red) and downregulated genes (green) (>2 fold). *Casp3* and *Casp8* are shown. (b) Real-time quantitative PCR was used to detect *Casp3* and *Casp8* expression in the lens at P1. (c, d) Whole mount *in situ* hybridization of *FoxE3* expression in embryonic development. *FoxE3* mRNA expression was dramatically reduced in the *Msx2*CKO lens vesicles compared with *Msx2*WT lens vesicles at E10.5 and E11.5.

mutants have previously shown varying degrees of microphthalmia with small lens formation or even aphakia and compromised laminar structure of the retina in severe cases.[14] Additionally, both germline *Msx2* knockouts and conditional *Msx2* knockouts exhibited small lens formation, while ocular phenotypes of germline knockouts were more severe; this can likely be explained by the different timings of *Msx2* deletions.[14] Different degrees of eye abnormalities in *Msx2*CKO could be caused by the timing of *Cre* induction (i.e., early vs. late) or the absolute level of *Cre* expression. The effective timing and dosage of *Cre* may also disrupt *Msx2* expression and downregulate *FoxE3* mRNA levels to different extents.

During the early stages of lens development in the present study (E9.5–E12.5), *Msx2*CKO mice showed small lens pits and lens vesicles, which may reflect reduced cellular proliferation and/or enhanced cell death. *Msxs*, *Bmp4*, and *Bmp7* regulate cell death during development by inducing the apoptosis of vertebrate retinal cells, neuronal precursors, and cranial neural crest cells.[15,33–37] In *Msx2*CKO embryos, the BrdU incorporation rate in central epithelia was significantly increased compared with *Msx2*WT littermates at E14.5. Notably enhanced apoptotic activity was

also observed from E10.5 in *Msx2*CKO embryos compared with *Msx2*WT littermates.

Microarray analysis identified DEGs in the *Msx2*CKO lens, and *Casp3* and *Casp8* were found to be significantly upregulated in the *Msx2*CKO lens at P1. An increase in *Casp8* activity could lead to stimulation of downstream *Casp3*, which subsequently activates the molecular cascade of apoptosis in LECs.[38,39] Our data together indicate that conditional deletion of *Msx2* in the lens induced apoptosis via the activation of *Casp3*/*Casp8* apoptosis signaling. However, our research was limited to microarray profiling of whole lens tissue at P1; gene expression profiling of early embryonic stages awaits further investigation.

In the present study, immunostaining revealed that *Sox2*, *Pax6*, and *AP2-α* expression patterns were the same as those reported earlier in the developing mouse eye (Figure S3).[40–47] However, *FoxE3* expression was significantly reduced (Figure 4c, 4d) and *Prox1* expression was upregulated in the lens vesicles of *Msx2*CKO mice (Figure S3). *Prox1* was previously shown to function downstream of *FoxE3* and its expression was suppressed by *FoxE3*. [30,48] Therefore, *Msx2* must be either parallel to or downstream from *Pax6*, *Sox2,* and *Ap2-α*, and to control *FoxE3* indirectly, and suppress *Prox1* either directly or indirectly.

Another abnormal feature of *Msx2*CKO mice is the lens stalk (corresponding to Peters anomaly in humans), resulting from failed separation of the cornea and the anterior lens epithelium.[49] *FoxE3* is involved in this process and is expressed in the early lens placode around E9 until it is turned off in differentiating primary lens fibers at E12.5.[48] In *FoxE3*$^{-/-}$ mice, the lens vesicle does not close and the lens remains irregular in shape and size with a persisting lens stalk.[48,50,51] The lack of separation may affect the distribution but not the intensity of cell adhesion molecules in the anterior lens epithelium, such as E- and N-cadherins.[50] This was observed in our current study in that the intensity of two adhesion molecules was identical between *Msx2*CKO and *Msx2*WT mice at E14.5. Moreover, nuclei displacement in lens fiber cells during lens differentiation can be explained by the involvement of *FoxE3* expression regulating the DnaseII-like acid Dnase (Dlad).[50] In *FoxE3* null mice, Dlad is significantly downregulated, resulting in cataract.[30,51,52]

In conclusion, the increased programmed cell death and cell proliferation alteration in the mouse lens may contribute to disorganized lens formation, resulting in microphthalmia in *Msx2*CKO mice. *Casp3* and *Casp8* are candidate signaling molecules regulating lens development in mice, and *Msx2* appears to function as an integrator in these signaling pathways, playing a crucial role during early lens development.

Acknowledgements

The authors thank Vardina Bensoussan and Yvan Lallemand for providing *Msx2*$^{fl/fl}$ mutant mice, and David Beebe and Peter Gruss for providing *Le-Cre* mice. The authors also thank Yi-Hsin Liu from the University of California for long-term cooperation.

Declaration of conflicting interests

The author(s) declared no potential conflicts of interest with respect to the research, authorship, and/or publication of this article.

Funding

The author(s) disclosed receipt of the following financial support for the research, authorship, and/or publication of this article: This work was supported by the National Natural Science Foundation of China (grant number: NSFC81371003), the China Postdoctoral Science Foundation (grant number: 2015M570517), the National Institutes of Health (grant number:

EY015417), and the Natural Science Foundation of Liaoning Province of China (grant number: 201602872).

ORCID iD

Jiangyue Zhao http://orcid.org/0000-0002-8065-3997

References

1. Bailey AP, Bhattacharyya S, Bronner-Fraser M, et al. Lens specification is the ground state of all sensory placodes, from which FGF promotes olfactory identity. *Dev Cell* 2006; 11: 505–517.
2. Sjodal M, Edlund T and Gunhaga L. Time of exposure to BMP signals plays a key role in the specification of the olfactory and lens placodes ex vivo. *Dev cell* 2007; 13: 141–149.
3. Lang RA. Pathways regulating lens induction in the mouse. *Int J Dev Biol* 2004; 48: 783–791.
4. Davidson D. The function and evolution of Msx genes: pointers and paradoxes. *Trends Genet* 1995; 11: 405–411.
5. Ekker M, Akimenko MA, Allende ML, et al. Relationships among msx gene structure and function in zebrafish and other vertebrates. *Mol Biol Evol* 1997; 14: 1008–1022.
6. Ramos C and Robert B. msh/Msx gene family in neural development. *Trends Genet* 2005; 21: 624–632.
7. Jabs EW, Muller U, Li X, et al. A mutation in the homeodomain of the human MSX2 gene in a family affected with autosomal dominant craniosynostosis. *Cell* 1993; 75: 443–450.
8. Liu YH, Kundu R, Wu L, et al. Premature suture closure and ectopic cranial bone in mice expressing Msx2 transgenes in the developing skull. *Proc Natl Acad Sci U S A* 1995; 92: 6137–6141.
9. Liu YH, Ma L, Kundu R, et al. Function of the Msx2 gene in the morphogenesis of the skull. *Ann N Y Acad Sci* 1996; 785: 48–58.
10. Liu YH, Tang Z, Kundu RK, et al. Msx2 gene dosage influences the number of proliferative osteogenic cells in growth centers of the developing murine skull: a possible mechanism for MSX2-mediated craniosynostosis in humans. *Dev Biol* 1999; 205: 260–274.
11. Jiang TX, Liu YH, Widelitz RB, et al. Epidermal dysplasia and abnormal hair follicles in transgenic mice overexpressing homeobox gene MSX-2. *J Invest Dermatol* 1999; 113: 230–237.
12. Satokata I, Ma L, Ohshima H, et al. Msx2 deficiency in mice causes pleiotropic defects in bone growth and ectodermal organ formation. *Nat Genet* 2000; 24: 391–395.
13. Wilkie AO, Tang Z, Elanko N, et al. Functional haploinsufficiency of the human homeobox gene MSX2 causes defects in skull ossification. *Nat Genet* 2000; 24: 387–90.
14. Zhao J, Kawai K, Wang H, et al. Loss of Msx2 function down-regulates the FoxE3 expression and results in anterior segment dysgenesis resembling Peters anomaly. *Am J Pathol* 2012; 180: 2230–2239.
15. Marazzi G, Wang Y and Sassoon D. Msx2 is a transcriptional regulator in the BMP4-mediated programmed cell death pathway. *Dev Biol* 1997; 186: 127–138.
16. Monaghan AP, Davidson DR, Sime C, et al. The Msh-like homeobox genes define domains in the developing vertebrate eye. *Development* 1991; 112: 1053–1061.
17. Holme RH, Thomson SJ and Davidson DR. Ectopic expression of Msx2 in chick retinal pigmented epithelium cultures suggests a role in patterning the optic vesicle. *Mech Dev* 2000; 91: 175–187.
18. Raucheman MCC, Luo P, Ma L, et al. Genetic interaction of Pax6 and Msx genes in lens induction (Abstract). *Dev biol* 1997; 186: B48.
19. Wu LY, Li M, Hinton DR, et al. Microphthalmia resulting from MSX2-induced apoptosis in the optic vesicle. *Invest Ophthalmol Vis Sci* 2003; 44: 2404–2412.
20. Faber SC, Robinson ML, Makarenkova HP, et al. Bmp signaling is required for development of primary lens fiber cells. *Development* 2002; 129: 3727–3737.
21. Furuta Y and Hogan BL. BMP4 is essential for lens induction in the mouse embryo. *Genes Dev* 1998; 12: 3764–3775.

22. Kamachi Y, Uchikawa M, Collignon J, et al. Involvement of Sox1, 2 and 3 in the early and subsequent molecular events of lens induction. *Development* 1998; 125: 2521–2532.
23. Wawersik S, Purcell P, Rauchman M, et al. BMP7 acts in murine lens placode development. *Dev Biol* 1999; 207: 176–188.
24. Ashery-Padan R, Marquardt T, Zhou X, et al. Pax6 activity in the lens primordium is required for lens formation and for correct placement of a single retina in the eye. *Genes Dev* 2000; 14: 2701–2711.
25. Soriano P. Generalized lacZ expression with the ROSA26 Cre reporter strain. *Nat Genet* 1999; 21: 70–71.
26. Bindea G, Mlecnik B, Hackl H, et al. ClueGO: a Cytoscape plug-in to decipher functionally grouped gene ontology and pathway annotation networks. *Bioinformatics* 2009; 25: 1091–1093.
27. Liu YH, Ma L, Wu LY, et al. Regulation of the Msx2 homeobox gene during mouse embryogenesis: a transgene with 439 bp of 5' flanking sequence is expressed exclusively in the apical ectodermal ridge of the developing limb. *Mech Dev* 1994; 48: 187–197.
28. Pizard A, Haramis A, Carrasco AE, et al. Whole-mount in situ hybridization and detection of RNAs in vertebrate embryos and isolated organs. *Curr Protoc Mol Biol* 2004; Chapter 14: Unit 14.9.
29. Shui YB, Arbeit JM, Johnson RS, et al. HIF-1: an age-dependent regulator of lens cell proliferation. *Invest Ophthalmol Vis Sci* 2008; 49: 4961–4970.
30. Medina-Martinez O, Brownell I, Amaya-Manzanares F, et al. Severe defects in proliferation and differentiation of lens cells in Foxe3 null mice. *Mol Cell Biol* 2005; 25: 8854–8863.
31. Wurm A, Sock E, Fuchshofer R, et al. Anterior segment dysgenesis in the eyes of mice deficient for the high-mobility-group transcription factor Sox11. *Exp Eye Res* 2008; 86: 895–907.
32. Manuel M, Pratt T, Liu M, et al. Overexpression of Pax6 results in microphthalmia, retinal dysplasia and defective retinal ganglion cell axon guidance. *BMC Dev Biol* 2008; 8: 59.
33. Trousse F, Esteve P and Bovolenta P. Bmp4 mediates apoptotic cell death in the developing chick eye. *J Neurosci* 2001; 21: 1292–1301.
34. Zhao S, Chen Q, Hung FC, et al. BMP signaling is required for development of the ciliary body. *Development* 2002; 129: 4435–4442.
35. Graham A, Francis-West P, Brickell P, et al. The signalling molecule BMP4 mediates apoptosis in the rhombencephalic neural crest. *Nature* 1994; 372: 684–686.
36. Takahashi K, Nuckolls GH, Tanaka O, et al. Adenovirus-mediated ectopic expression of Msx2 in even-numbered rhombomeres induces apoptotic elimination of cranial neural crest cells in ovo. *Development* 1998; 125: 1627–1635.
37. Furuta Y, Piston DW and Hogan BL. Bone morphogenetic proteins (BMPs) as regulators of dorsal forebrain development. *Development* 1997; 124: 2203–2212.
38. Ma T, Chen T, Li P, et al. Heme oxygenase-1 (HO-1) protects human lens epithelial cells (SRA01/04) against hydrogen peroxide (H2O2)-induced oxidative stress and apoptosis. *Exp Eye Res* 2016; 146: 318–329.
39. Zhu L, Zhao K and Lou D. Apoptosis factors of lens epithelial cells responsible for cataractogenesis in vitrectomized eyes with silicone oil tamponade. *Med Sci Monit* 2016; 22: 788–796.
40. Kammandel B, Chowdhury K, Stoykova A, et al. Distinct cis-essential modules direct the time-space pattern of the Pax6 gene activity. *Dev Biol* 1999; 205: 79–97.
41. Grindley ND and Leschziner AE. DNA transposition: from a black box to a color monitor. *Cell* 1995; 83: 1063–1066.
42. Kamachi Y, Uchikawa M, Tanouchi A, et al. Pax6 and SOX2 form a co-DNA-binding partner complex that regulates initiation of lens development. *Genes Dev* 2001; 15: 1272–1286.
43. Glaser T, Jepeal L, Edwards JG, et al. PAX6 gene dosage effect in a family with congenital cataracts, aniridia, anophthalmia and central nervous system defects. *Nat Genet* 1994; 7: 463–471.
44. Oliver G, Sosa-Pineda B, Geisendorf S, et al. Prox 1, a prospero-related homeobox gene

expressed during mouse development. *Mech Dev* 1993; 44: 3–16.
45. Wigle JT, Chowdhury K, Gruss P, et al. Prox1 function is crucial for mouse lens-fibre elongation. *Nat Genet* 1999; 21: 318–322.
46. Makhani LF, Williams T and West-Mays JA. Genetic analysis indicates that transcription factors AP-2alpha and Pax6 cooperate in the normal patterning and morphogenesis of the lens. *Mol Vis* 2007; 13: 1215–1225.
47. West-Mays JA, Zhang J, Nottoli T, et al. AP-2alpha transcription factor is required for early morphogenesis of the lens vesicle. *Dev Biol* 1999; 206: 46–62.
48. Blixt A, Mahlapuu M, Aitola M, et al. A forkhead gene, FoxE3, is essential for lens epithelial proliferation and closure of the lens vesicle. *Genes Dev* 2000; 14: 245–254.
49. Ozeki H, Ogura Y, Hirabayashi Y, et al. Suppression of lens stalk cell apoptosis by hyaluronic acid leads to faulty separation of the lens vesicle. *Exp Eye Res* 2001; 72: 63–70.
50. Blixt A, Landgren H, Johansson BR, et al. Foxe3 is required for morphogenesis and differentiation of the anterior segment of the eye and is sensitive to Pax6 gene dosage. *Dev Biol* 2007; 302: 218–229.
51. Nishimoto S, Kawane K, Watanabe-Fukunaga R, et al. Nuclear cataract caused by a lack of DNA degradation in the mouse eye lens. *Nature* 2003; 424: 1071–1074.
52. Medina-Martinez O and Jamrich M. Foxe view of lens development and disease. *Development* 2007; 134: 1455–1463.